ISSN: 0067-2904
GIF: 0.851

Theoretical Studies of Corrosion Inhibition Efficiency of Two New N-Phenyl-Ethylidene-5-Bromo Isatin Derivatives

Rehab Majed Kubba*, Mustafa Mohammed Khathem
Department of Chemistry, College of Science, University of Baghdad, Baghdad, Iraq

Abstract:

PM3 and DFT (B3LYP) with a 6-311++G (2d, 2p) level of theoretical quantum mechanical calculations were employed to give investigation into the inhibition efficiency of the two new N-phenyl-ethylidene-5-bromo isatin derivatives which are N-phenyl-ethylidene-5-bromo-3[(imine aceto) urea]-2-oxo indole (NPEO) and N-phenyl-ethyeidine-5-bromo-3[(imine aceto) thiourea]-2-oxo indole (NPES). The calculated physical properties and quantum chemical parameters correlated to the inhibition efficiency all are studied and discussed at the equilibrium geometry in a vacuum, dimethyl sulfoxide and aqueous at their correct symmetry.

Keywords: corrosion inhibitor, theoretical, PM3, DFT, N-benzyl-5-Bromo Isatin derivatives.

دراسة نظرية لكفاءة تثبيط تآكل حديد الصلب الكاربوني بفعل مشتقين جديدين من مشتقات N–فنيل أثيليدين–5–برومو إيساتين

رحاب ماجد كبة*، مصطفى محمد كاظم
قسم الكيمياء، كلية العلوم، جامعة بغداد، بغداد، العراق

الخلاصة

تضمن البحث استخدام حسابات ميكانيك الكم العائدة لنظريتي PM3 ونظرية دوال الكثافة DFT عند مستوى الحساب (B3LYP) 6-311++G (2d, 2p) وباستخدام برنامج Gaussian–09 في حساب الشكل الهندسي التوازني لمشتقين جديدين من N- فنيل اثيليدين–5– برومو ايساتين هما N- فنيل اثيليدين— 5- برومو-3-[(إيمينو اسيتو) يوريا]-2-اوكسو إندول (NPEO) وN- فنيل اثيليدين-5-برومو-3-[(إيمينو اسيتو) ثايو يوريا]-2-اوكسو إندول (NPES). تم حساب ومناقشة الصفات الفيزياوية ومعاملات ميكانيك الكم المرتبطة بدراسة كفاءة هذه المركبات كمثبطات تآكل عند الشكل الهندسي التوازني في الفراغ وفي مذيبي ثنائي مثيل سلفوكساييد والماء وعند التماثل الصحيح لهذه الجزيئات.

Introduction:

Isatin (1H-indol-2,3-dione) compounds are of great synthetic versatility to use in the preparation of various heterocyclic systems such as quinoline and indole derivatives making them important raw materials for drug synthesis. Isatin have also been found in mammalian tissues, which has raised interest in their study as modulators in various biochemical processes. Isatin (1H-indole-2,3-dione) derivatives are synthetically versatile substrates, where they can be used for the synthesis of a large variety of heterocyclic compounds, such as indoles and quinolines, and the raw materials for drug synthesis. The advances in the use of isatin for organic synthesis during the last twenty-five years, as well as survey of its biological and pharmacological properties were reported in many researches and in the accompanying supplementary information [1]. The biological and pharmacological properties of isatin and its derivatives have led to extensive use of these compounds as key intermediates in organic synthesis. Isatin is a core constituent of many alkaloids and drugs as well as dyes, pesticides and

*Email: Rehab_ mmr_kb@yahoo.com

analytical reagents. Literature surveys reveal that various derivatives of isatin possess diverse activities such as antibacterial, antifungal, antiviral, anti-HIV, anti-mycrobacterial, anticancer, anti-inflammatory and anticonvulsant activities [2].

Fundamental reactivity of isatin and its derivatives is the presence of several reaction centers in their structures which made them capable of participating in a large number of reactions. The keto group at position 2 and particularly at position 3 can enter into addition reactions at the C-O bond and into condensation reactions. Through the amide group, compounds of the isatin series are capable of entering into N-alkylation and N-acylation and into Mannich and Michael reactions [3-5].

Corrosion of metallic surfaces [6] can be controlled or reduced by the addition of chemical compounds to the corroding. This form of corrosion control is called inhibition and the compounds added are known as corrosion inhibitors, which is one of the most common effective and economic methods to protect metals especially in acid media [7-8].

One of the most important methods in the protection metal against corrosion is the use of organic inhibitors. Organic compounds containing heteroatoms including nitrogen, sulfur, and oxygen [9] have been reported to inhibit metal corrosion. The inhibiting action of these organic compounds is usually attributed to their interactions with the metal surface via their adsorption. Polar functional groups are regarded as the reaction center that stabilizes the adsorption process [10].

Quantum chemical calculations have been proved to be a very powerful tool for studying corrosion inhibition mechanism [11-15]. Density functional theory (DFT) [16] has provided a very useful framework for developing new criteria for rationalizing, predicting, and eventually understanding many aspects of chemical processes [17]. A variety of chemical concepts which are now widely used as descriptors of chemical reactivity, e.g., electronegativity [18] hardness or softness quantities etc., appear naturally within DFT [19]. A number of excluded parameters that should be involved include the effect of solvent molecules, surface nature, and adsorption sites of the metal atoms or oxide sites or vacancies, competitive adsorption with other chemical species in the fluid phase and solubility [12].

The aim of this work is to study the corrosion inhibition efficiency parameters of the two newly prepared derivatives of N-benzyl-5-bromo isatin Figure-1 which were fixed among many newly prepared derivatives of 5-bromo isatin derivatives [20], depending on studying their quantum mechanical calculations for corrosion inhibition efficiency as a best corrosion inhibitor than the others by using PM3 and DFT methods.

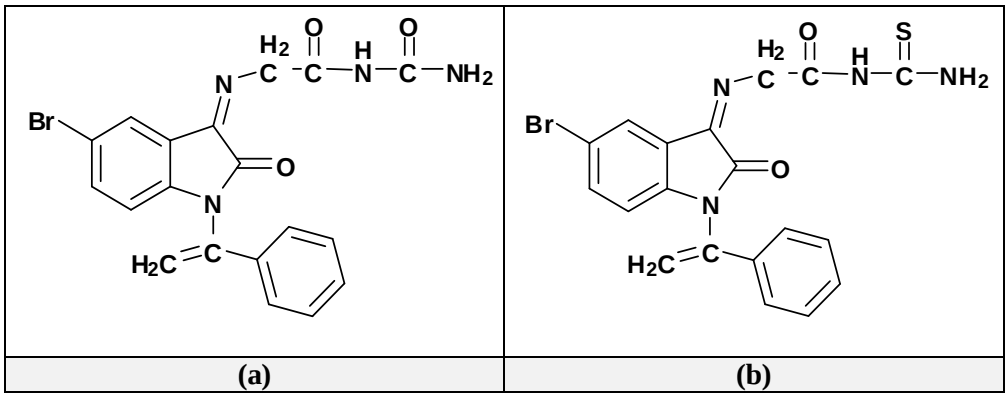

Figure 1- Chemical structure of **a-** N-phenyl-ethyledine-5-bromo-3-[(imine aceto) urea]-2-oxo indole, **b-** N-phenyl-ethyledine-5-bromo-3-[(imine aceto) thiourea]-2-oxo indole.

Results and Discussion:

Molecular geometry

The molecules were built with the Gauss View 09 implemented in Gaussian 09 package [21], their corresponding geometries were fully optimized using PM3 semiempirical method and Density Functional Theory (DFT) which was carried out using Becke′s three-parameter functional and the correlation functional of Lee, Yang and Parr (B3LYP) with a 6-311++G (2d, 2p) level of theory [22,23,16], and the vibrational calculations probe that their equilibrium structures correspond to the minima energy for N-benzyl-5-bromo isatin derivatives (absence of imaginary frequencies).The geometries of the investigated molecules were re-optimized in dimethyl sulfoxide and aqueous at the

same level of DFT theory. The final geometries of **NPEO** and **NPES** corresponding to DFT method are given in Figure-2.

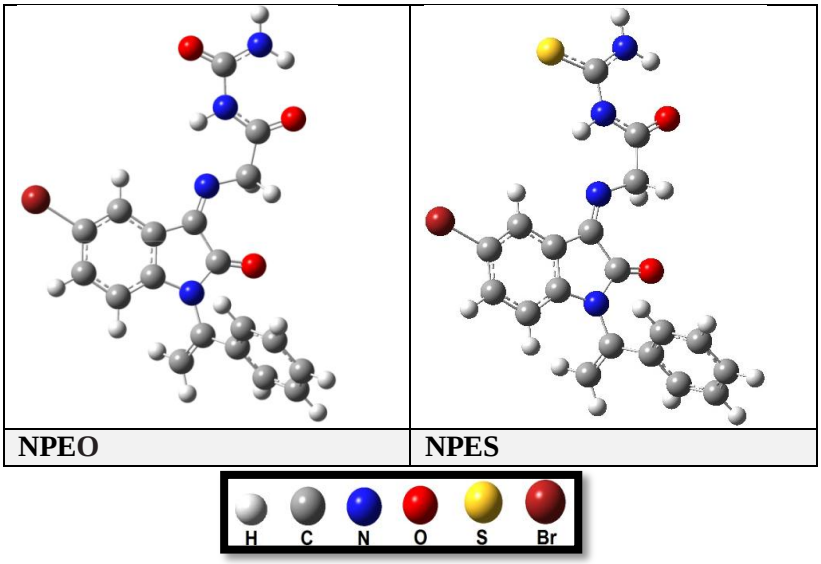

Figure 2- Equilibrium geometry of the inhibitors molecules calculated by PM3 and DFT (B3LYP/6-311++G (2d, 2p)) methods.

It is observed from the computational results that the substitution of O atom in **NPEO** by S atom in **NPES** involves significant modifications on the structural parameters such as bond distances, bond angles and dihedral angles of the studied inhibitors, Table-1a,1b. Figure-3 shows the label of the atoms of the studied inhibitors.The comparison between the optimized geometrical structures of **NPEO** and **NPES** compounds in vacuum showed that the bond length N1-C2, C2-C8, C5-Br, C15-C14, C15-C16, C18-C19, C19-N12 are shorter in **NPES** than in **NPEO** by about (0.001-0,022)A and the N1-C10, C2-C3 bonds in **NPES** are longer than the single **NPEO** by about 0.001A,.

These differences can be explained by the delocalization in O17=C16-N18 region more in **NPES** compound. Large values of the bond lengths were observed for C19=S20 in **NPES** and for C5-Br in both **NPEO and NPES**. For this, it can be concluded that the adsorption on a metallic surface is clearly easy with C19=S20 and C5-Br for **NPES** only with C5-Br for **NPEO**. The compounds under investigation are not planar, this result is confirmed by the values of the C2-N1-C10 for both NPEO and NPES compounds Tables-1a,1b. The values of cis dihedral angles (N14C15C16N18, O17C16N18C19, C16N18C19N21, O20C19N21H22) and trans dihedral angles (N14C15C16O17, C15C16N18C19, C16N18C19O20, O17C16N18H) show that the molecule is bent at this part for **NPEO** and very close to planner for **NPES**. This result explains that the adsorption on the metallic surface was easier for **NPES** than **NPEO**.

In addition, it is noticed that there are slightly solvent effect (increase by 0.0001) on some bond lengths, bonds angles and dihedrals angles.

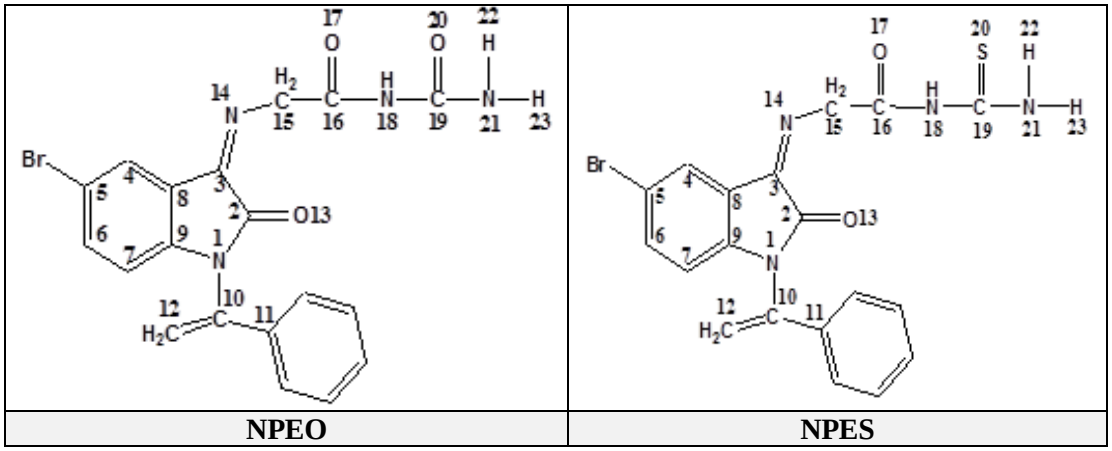

Figure 3- Label of **NPEO** and **NPES** inhibitor compounds.

Table 1a- Calculated geometric structure for **NPEO** molecule by using DFT method in the three media (vacuum, DMSO and H_2O).

Description Bond length	Bond length (Å)	Description angle (^{0})	Angle (^{0})	Description Dihedral angle (^{0})	Dihedral angle (^{0})
N1-C2	1.397	C2N1C9	110.209	C2N1C10C12	-120.794
N1-C9	1.426	C2N1C10	123.478	C2N1C10C11	60.936
N1-C10	1.440	N1C2C3	106.453	C10N1C2O13	0.577
C2-C3	1.522	N1C2C13	126.460	O13C2C3N14	-2.622
C2=O13	1.239	C2C3C8	105.780	C2C3N14C15	-0.879
C3-C8	1.464	C2C3C14	128.007	N14C15C16O17	171.274
C3-N14	1.282	C8C4C5	117.851	N14C15C16N18	-9.239
C4-C5	1.394	C4C5C6	121.442	C15C16N18C19	-178.65
C4-C8	1.390	C4C5Br	119.278	O17C16N18C19	0.801
C5-C6	1.395	C6C7C9	117.871	C16N18C19O20	179.783
C5-Br	1.950	C3C8C4	131.159	C16N18C19N21	-0.225
C6-C7	1.402	N1C9C7	129.242	O20C19N21H22	-0.333
C7-C9	1.387	N1C9C8	109.601	O20C19N21H23	-179.689
N14-C15	1.466	N1C10C11	116.032	O17C16N18H	-178.310
C15-C16	1.520	N1C10C12	119.541		
C16=O17	1.251	C3N14C15	123.226		
C16-N18	1.368	C14N15C16	111.556		
N18-C19	1.420	C15C16O17	119.939		
C19=O20	1.247	C15C16N18	115.540		
C19-N21	1.356	N18C19S20	119.164		
N21-H	1.003	N18C19N21	115.586		

Table 1b- Calculated geometric structure for **NPES** molecule by using DFT method in the three media (vacuum, DMSO and H_2O).

Description Bond length	Bond length (Å)	Description angle (^{0})	Angle (^{0})	Description Dihedral angle (^{0})	Dihedral angle (^{0})
N1-C2	1.395	C2N1C9	110.197	C2N1C10C12	-119.088
N1-C9	1.426	C2N1C10	123.620	C2N1C10C11	62.499
N1-C10	1.441	N1C2C3	106.470	C10N1C2C13	0.230
C2-C3	1.521	N1C2C13	126.741	C13C2C3N14	-1.590
C2=O13	1.239	C2C3C8	105.861	C2C3N14C15	-0.179
C3-C8	1.463	C2C3C14	127.630	N14C15C16O17	179.701
C3-N14	1.282	C8C4C5	117.821	N14C15C16N18	-0.313
C4-C5	1.394	C4C5C6	121.441	C15C16N18C19	-179.954
C4-C8	1.390	C4C5Br	119.225	O17C16N18C19	0.030
C5-C6	1.395	C6C7C9	117.838	C16N18C19S20	-179.913
C5-Br	1.949	C3C8C4	131.231	C16N18C19N21	0.058
C6-C7	1.402	N1C9C7	129.223	S20C19N21H22	0.039
C7-C9	1.387	N1C9C8	109.625	S20C19N21H23	-179.945
N14-C15	1.466	N1C10C11	116.096	O17C16N18H	-179.888
C15-C16	1.517	N1C10C12	119.192		
C16=O17	1.252	C3N14C15	123.058		
C16-N18	1.373	C14N15C16	111.271		
N18-C19	1.398	C15C16O17	120.307		
C19=S20	1.720	C15C16N18	115.381		
C19-N21	1.341	N18C19S20	119.461		
N21-H	1.004	N18C19N21	116.031		

Global molecular reactivity

Frontier orbital theory is useful in predicting adsorption centers of the inhibitor molecules responsible of the interaction metallic surface/molecule [24]. The terms involving the Frontier Molecular Orbital (FMO) could provide a dominative contribution, because of the inverse dependence of stabilization energy on orbital energy difference ($\Delta E= E_{LUMO}-E_{HOMO}$).

The HOMO energy (E_{HOMO}) is often associated to the electron donating ability of the molecule; therefore, inhibitors with high values of E_{HOMO} have a tendency to donate electrons to appropriate acceptor with low empty molecular orbital energy. Conversely, the LUMO energy (E_{LUMO}) indicates the electron-accepting ability of the molecule, the lowest its value the higher the capability of accepting electrons. The gap energy between the Frontier orbitals (ΔE) is another important factor in describing the molecular activity, so when the gap energy decreased, the inhibitor efficiency is improved [25].

The calculated quantum chemical parameters related to the inhibition efficiency of the studied molecule, such as the highest occupied molecular orbital (E_{HOMO}), energy of the lowest unoccupied molecular orbital (E_{LUMO}), energy gap ($\Delta E= E_{LUMO}-E_{HOMO}$), dipole moment ($\mu$), the electronegativity (χ), the ionization potential (IP), the electron, affinity (EA), the global hardness (**S**), and the fraction of electron transfer (ΔN) from the inhibitor molecules to iron, are collected in Tables-2a,2b and Tables-3a,3b,4a,4b for inhibitors with both PM3 and DFT method.

According to Koopman's theorem [26], the ionization potential (IE) and electron affinity (EA) of the inhibitors are calculated using the following equations and hence χ and μ are calculated.

IE (Ionization potential)= $-E_{HOMO}$ **(1)**

EA (Electron affinity)= $-E_{LUMO}$ **(2)**

Hardness (η) has been defined as the second derivative of the E with respect to N as $\nu(r)$ property which measures both the stability and reactivity of the molecule [27].

η(Hardness) $=(\partial^2 E/\partial N^2)\nu(r)\eta =$**(IE - EA)/ 2** **(3)**

χ(Electronegativity)= -μ= $-(\partial E/\partial \Lambda)\nu(\rho) = (IE + EA)/2$ **(4)**

Where $\nu(r)$ and μ are, respectively, the external and electronic chemical potentials.

The higher HOMO energy corresponds to the more reactive molecule in the reactions with electrophiles, while lower LUMO energy is essential for molecular reactions with nucleophiles.

The global softness (S) is the inverse of the global hardness [28].

S (global softness) = 1/ η **(5)**

Global electrophilicity index (ω) introduced by Parr [29], calculated using the electronegativity and chemical hardness parameters through the equation 6: A high value of electrophilicity describes a good electrophile while a small value of electrophilicity describes a good nucleophile [30]. In Table-3 the high value of ω, (4.299eV) indicates the better corrosion inhibition efficiency.

Global electrophilicity index (ω)= $(-x)^2/2\eta = \mu^2/2\eta$ **(6)**

The fraction of electrons transferred (ΔN) from an inhibitor to carbon steel surface was also calculated using a theoretical χFe and η_{Fe} values for mild steel of 7.0 eV mol^{-1} and 0.0 eV mol^{-1}, respectively [31]. The ΔN values are correlated to the inhibition efficiency resulting from electron donation. According to Lukovits et al. study [32], if $\Delta N < 3.6$, the inhibition efficiency increases with increasing electron- donating ability at the metal surface. The obtained values of ΔN reported in Table 3b according to PM3 and Table 4b according to DFT; show that the **NPES** have the highest value of ΔN in the gas and solvent phase. Therefore, the highest inhibition efficiency contemplate experimentally for NPES by the tendency of molecule to receive the electron by S atom in unoccupied orbital (3d). This ability to receive the electron from the metallic surface increases the inhibition efficiency [33].

When two systems, Fe, and inhibitor, are brought together, electrons will flow from lower χ(inhibitor) to higher χ(Fe), until the chemical potentials become equal. The number of transferred electrons (ΔN) was also calculated [34] by using the equation below.

ΔN (Electron transferred) = (χ_{Fe} - $\chi_{inhib.}$)/ [2 (η_{Fe} +$\eta_{inhib.}$)] **(7)**

Where χ_{Fe} and χ_{inh} denote the absolute electronegativity of iron and inhibitor molecule respectively η_{Fe} and η_{inh} denote the absolute hardness of iron and the inhibitor molecule respectively.

The dipole moment (μ in Debye) is another very important electronic parameter that results from the non uniform distribution of charges on the various atoms in the molecule. The high value of dipole moment increases the adsorption between a chemical compound and metal surface [35].

The dipole moment provides information on the polarity of the whole molecule. High dipole moment values are reported to facilitate adsorption and therefore inhibition by influencing the transport process through the adsorbed layer. Several authors have stated that the inhibition efficiency increases with dipole moments values [36-38].The dipole moments of **NPEO** and **NPES** are (5.0031, 6.4274 Debye), in the gas phase for PM3 method and (6.5301, 7.2966 Debye) for DFT method Tables-2a,3a, 4a respectively, increasing in dimethyl sulfoxide and aqueus solution. The high dipole moment value of these compounds probably indicates strong dipole-dipole interactions between them and metallic surface. Accordingly, the N-phenyl-ethylidene-5-bromo isatin derivatives adsorption in aqueous solution can be regarded as a quasi-substitution process of the DMSO and water molecules by the inhibitors molecules at the metal surface (H_2O ads). The higher value, of the calculated μ and other parameters efficiency of the inhibitor molecule **NPES** enumerates its better inhibition efficiency than **NPEO** in the gas phase and both solvents H_2O and DMSO at DFT calculations Tables-3a, 3b, 4a, 4b, even so PM3 calculations in the gas phase Tables-2a,2b.

The calculated quantum chemical parameters in the presence of solvent (dimethyl sulfoxide, water) had shown a good effect for increasing the efficiency inhibition for **NPEO** Tables-3a,3b, with slight decrease in efficiency inhibition for **NPES** Tables-4a,4b, but even though as a whole results, **NPES** has a better efficiency inhibition parameters in solvent than that of **NPEO** inhibitor.

Table 2a- PM3 calculated for some physical properties of the inhibitor molecules at the equilibrium geometries.

Inhib.	M. formula M. wt. (gm/mol)	ΔH^0_f (kcal/mol) (kJ/mol)	E_{HOMO} (eV)	E_{LUMO} (eV)	$\Delta E_{HOMO-LUMO}$ (eV)	μ (Debye)
NPEO (Gas)	$C_{19}H_{15}N_4O_3Br$ 427.257	-3.557 -14.883	-9.7691	-1.3333	8.4358	5.0031
NPES (Gas)	$C_{19}H_{15}N_4O_2SBr$ 443.317	58.795 245.999	-8.9527	-1.3878	7.5649	6.4274

Table 2b- Quantum chemical parameters for the inhibitor molecules as calculated using PM3 method.

Inhib.	IE (eV)	EA (eV)	η (eV)	χ (eV)	S (eV)	**ω** (eV)	ΔN
NPEO (Gas)	9.7691	1.3333	4.2179	5.5512	0.2370	3.6529	0.1717
NPES (Gas)	8.9527	1.3878	3.7824	5.1702	0.2643	3.5335	0.2418

Table 3a- DFT calculated for some physical properties of the **NPEO** inhibitor molecule in the three media (vacuum, DMSO, and H_2O) at the equilibrium geometries.

Inhib.	Sym.	E_{HOMO} (eV)	E_{LUMO} (eV)	$\Delta E_{HOMO-LUMO}$ (eV)	μ (Debye)	E_{total} (eV)
NPEO (Gas)	C_1	-6.6628	-3.3051	3.3576	6.5301	-102106.526
NPEO (DMS)	C_1	-6.4620	-3.1200	3.3420	7.8349	-102107.108
NPEO (H2O)	C_1	-6.4598	-3.1176	3.3422	7.8546	-102107.118

Table 3b- Quantum chemical parameters for the **NPEO** inhibitor molecule in the three media (vacuum, DMSO, and H_2O) as calculated using DFT method.

Inhib.	IE (eV)	EA (eV)	η(eV)	χ (eV)	S (eV)	**ω** (eV)	ΔN
NPEO (Gas)	6.6628	3.3051	1.6788	4.9840	0.5956	7.3980	0.6004
NPEO (DMS)	6.4620	3.1200	1.6709	4.7910	0.5984	6.8683	0.6609
NPEO (H_2O)	6.4598	3.1176	1.6710	4.7887	0.5984	6.8614	0.6616

Table 4a- DFT calculated for some physical properties of the **NPES** inhibitor molecule in the three media (vacuum, DMSO, and H_2O) at the equilibrium geometries.

Inhib.	Sym.	E_{HOMO} (eV)	E_{LUMO} (eV)	$\Delta E_{HOMO-LUMO}$ (eV)	μ (Debye)	E_{total} (eV)
NPES (Gas)	C_1	-5.9624	-3.3598	2.6025	7.2966	-110894.730
NPES (DMSO)	C_1	-6.4780	-3.1527	3.3253	8.8759	-110895.308
NPES (H_2O)	C_1	-6.4761	-3.1500	3.3261	8.8981	-110895.319

Table 4b- Quantum chemical parameters for the **NPES** inhibitor molecule in the three media (vacuum, DMSO, and H_2O) as calculated using DFT method.

Inhib.	IE (eV)	EA (eV)	η(eV)	χ (eV)	S (eV)	**ω** (eV)	ΔN
NPES (Gas)	5.9624	3.3598	1.3012	4.6611	0.7684	8.3481	0.8986
NPES (DMSO)	6.4780	3.1527	1.6626	4.8153	0.6014	6.9609	0.6569
NPES (H_2O)	6.4761	3.1500	1.6630	4.8131	0.6013	6.9649	0.6574

The optimized geometries of the studied compounds in the neutral form including their HOMO and LUMO distributions density are shown in Figure-4. It can be seen that **NPEO** and **NPES** have a similar HOMO and LUMO distribution. For HOMO are all mainly located on the 3[(imine aceto) thiourea]-2-oxo indole in **NPES** moiety and 3[(imine aceto) urea]-2-oxo indole in **NPEO** moiety.

These results indicate that the interaction between these molecules and the carbon steel surface concerns their moieties. In addition, the LUMO electronic density for both NPEO and NPES was distributed on their isatin ring and imine aceto moiety.

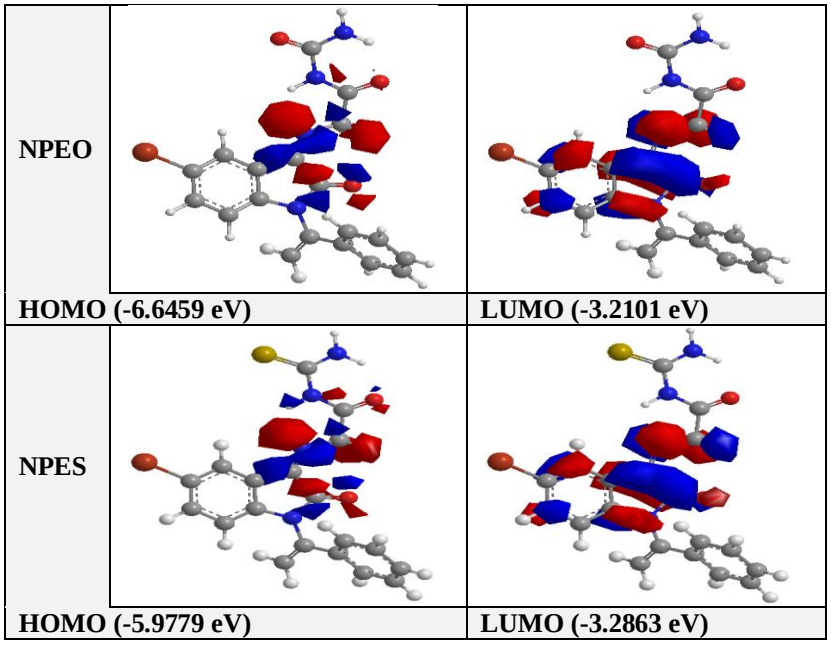

Figure 4- The Frontier Molecule Orbital density distributions of N-benzyl-5-bromo-3- [(imine aceto) urea]-2-oxo indole, and N-benzyl-5-bromo-3- [(imine aceto) thiourea]-2-oxo indole as calculating using DFT method. Red color indicates the negatively charged lobe, blue color indicates the positively charge lobe:

Active sites

For the purpose of establishing the active sites of the inhibitor calculated molecules, three influencing factors: natural atomic charge, distribution of frontier molecular orbital and indices. According to classical chemical theory, all chemical interactions are either by electrostatic or orbital interactions. Electrical charges in the molecule were obviously the driving force of electrostatic

interactions. It is proven that local electric densities or charges are important in many chemical reactions and physicochemical properties of compound [39-41]. According to Table-5, the favored sites for nucleophilic attack and the most reactive sites of **NPEO** that have the highest negative charge center and could offer electrons to the Fe atoms to form coordinate bond are C4, C5, C6, C7, C12, O13 atoms of the N-bensyl-5-bromo isatin rings, and N14, O17, N18, O20, N21 hetero atoms.

Table 5-DFT Mulliken charges population analysis for the calculated inhibitor molecules NPEO and NPES in the three media (vacuum, DMSO, and H_2O).

Atom	Electronic charge		Atom	Electronic charge	
	NPEO	NPES.		NPEO	NPES.
N1	-0.047 G -0.003 D -0.002 W	-0.060 G -0.016 D -0.015 W	C12	-0.359 G -0.336 D -0.336 W	-0.375 G -0.354 D -0.353 W
C2	0.078 G 0.164 D 0.166 W	0.031 G 0.116 D 0.118 W	O13	-0.414 G -0.495 D -0.496 W	-0.412 G -0.492 D -0.494 W
C3	0.043 G 0.042 D 0.042 W	0.093G 0.100 D 0.100 W	N14	-0.251 G -0.251 D -0.250 W	-0.244 G -0.246 D -0.245 W
C4	-0.116 G -0.107 D -0.107 W	-0.056 G -0.056 D -0.056 W	C15	0.117 G 0.107 D 0.107 W	0.140 G 0.121 D 0.120 W
C5	-0.128 G -0.140 D -0.140 W	-0.104 G -0.114 D -0.114 W	C16	0.069 G 0.118 D 0.119 W	0.093 G 0.139 D 0.140 W
Br	-0.054 G -0.074 D -0.074 W	0.049 G -0.070 D -0.070 W	O17	-0.505 G -0.566 D -0.567 W	-0.486 G -0.537 D -0.538 W
C6	-0.422 G -0.409 D -0.409 W	-0.422 G -0.411 D -0.411 W	N18	-0.421 G -0.408 D -0.408 W	-0.284 G -0.273 D -0.272 W
C7	-0.273 G -0.263 D -0.263 W	-0.273 G -0.265 D -0.265 W	C19	0.625 G 0.663 D 0.663 W	0.494 G 0.520 D 0.520 W
C8	0.225 G 0.228 D 0.228 W	0.208 G 0.190 D 0.189 W	O20	-0.509 G -0.592 D -0.593 W	--------
C9	0.345 G 0.333 D 0.333 W	0.303 G 0.294 D 0.294 W	S20	-------	-0.516 G -0.616 D -0.618 W
C10	-0.011 G -0.031 D -0.032 W	0.034 G 0.012 D 0.012 W	N21	-0.289 G -0.304 D -0.304 W	-0.240 G -0.244 D -0.244 W
C11	1.048 G 0.924 D 0.921 W	0.970 G 0.851 D 0.847 W			

G: gas phase, D: dimethyl sulfoxide (DMSO), W: water, violet color: increase in electronic charge, red color: decrease in electronic charge.

For **NPES**, there are the same reactive sites except S20 atom instead of O20 heteroatom. For the electrophilic attack the most reactive sites of **NPEO** at which have the highest positive charge are C8, C2, C9, C11, C15 and C19 atoms. For **NPES,** the sites which can accept the electron are the same atoms as for **NPEO**, which are C8, C2, C9, C11, C15 and C19 atoms. These centers can accept electrons from 3d orbital's of the Fe atom to form feedback bond, thus further strengthening the interaction of inhibitor and Fe surface. Based on the discussion above, it can be concluded that **NPEO** and NPES have many active centers for adsorption on carbon steel surface. Thus, the areas containing N, O and S atoms are the most favored sites for bonding to carbon steel surface through donating electrons. However, the S atom can give and receive the electron to and from metal, respectively because it has a lone pair of electrons and unfilled d orbital's. In addition, the active sites area for

NPES is observed to be a nearly planner while for **NPEO** inhibitor is clearly bent. Tables-1a,1b and Figure-5. This leads for **NPES** to be adsorb easier by donating electrons to metallic surface in agreement with experimental results of other research [37]. The last process reinforces the inhibitor molecule adsorption on a metallic surface and the both process are more accentuated in **NPES** than in **NPEO**.

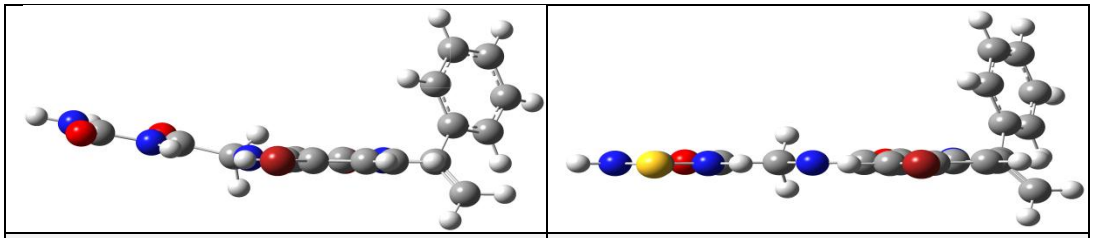

NPEO	**NPES**

Figure 5- Surface area plane of the active sites of the calculated inhibitors.

Taking into account the solvent effect Table-5, the electronic charge for the nucleophilic and electrophilic attack increases slightly (0.012-0.020) for both NPEO and NPES on C5, Br, C10, C12, C19 and increases (0.048-0.102) on C2, O13, C16, O17, C19, O20 (**NPEO**), S20 (**NPES**), N21. The highest increasing value is on S20 for **NPES** (0.102) in the aqueous phase. The partial charges on the individual atoms in a molecule also indicate the reactive centers for a particular inhibitor. Atoms with the highest negative charge are considered to have an electron donor role when interacting with metal surfaces. In solution, the electronic charge decreases on N1, C4, C6, C9, C11, C12, C15, N18. The highest decreasing value on C11 for **NPEO** (0.122, 0.127) in DMSO and aqueous, (0.119, 0.123) for **NPES** in DMSO and aqueous respectively.

The electronic charge values for the nucleophilic and electrophilic attack of NPEO and NPES are stronger in solution than in gas phase. From this analysis, it is obvious that in the aqueous solution, the S atom is more likely to be a site for nucleophilic attack in NPES than in gas phase and this leads to easy adsorb by donating electron from NPES to a metallic surface. The Mulliken atomic charges population analysis for the calculated inhibitor molecules NPEO and **NPES** in the three media (vacuum, DMSO, and H_2O) are listed in Table -5.

Conclusion

The inhibition efficiency of carbon steel corrosion by N-benzyl-5-bromo isatin derivatives has been investigated using quantum chemical calculations using PM3 semiempirical method and (DFT/B3LYP/6-311++G (2d, 2p)) level of theory. The following conclusions were drawn from this study:

1. The geometrical parameters with both PM3 and DFT methods show that the inhibitor molecule is efficient for the corrosion inhibition.
2. A good correlation was found between the quantum chemical parameters calculating by PM3 and DFT (E_{HOMO}, E_{LUMO}, gap energy (ΔE), dipole moment (μ)) -----etc., with inhibition efficiency. This can be explained by the fact that the inhibitor compound can accept and donor electrons from the metal, and these processes reinforce the adsorption of the inhibitor molecules on carbon steel surface.
3. The density distributions of the frontier molecular orbitals (HOMO and LUMO) show that N-benzyl-5-bromo isatin derivatives adsorb through the active centers nitrogen, oxygen, sulfur and π electrons of the isatin ring and other heteroatoms.
4. The reactive site for electrophilic and nucleophilic attacks, determined correctly by the DFT Mulliken charges population analysis for the calculated inhibitor molecule.
5. The geometrical structures show that the active sites surface area for NPES molecule is more planar than for NPEO, thus, the first one is the most efficient for the corrosion inhibition. This result is in good agreement with experimental results**.**

References:

1. Da Silva, J.F.M., Garden, S.J. and Pinto, A.C. **2001.** The chemistry of isatin: reviews from [1975 to 1999], *J. Braz. Chem. Soc*., 12(3), pp: 273-324.
2. Lashgari, N. and Ziarani, G.M. **2012**. Synthesis of heterocyclic compounds based on isatin through 1,3-dipolar cycloaddition reactions. *ARKIVOC (Archive for organic chemistry)*, 1, pp:

277-320.

3. Sumpter, W.C. **1944**. The chemistry of isatin. *Chemical Reviews*, 34(3), pp: 393–434.

4. Sonawane, R.P. and Tripathi, R.R. **2013**. The chemistry and synthesis of 1H-indole-2,3-dione (isatin) and its derivatives. *International Letters of Chemistry, Physics, and Astronomy*, 7(1), pp: 30-36.

5. Pakravan, P., Kashanian, S., Khodaei, M.M. and Harding, F.J. **2013**. Biochemical and pharmacological characterization of isatin and its derivatives: from structure to activity. *Pharmacological Reports*, 65, pp: 313-335.

6. Bentiss, F., Lebrini, M. and Lagrenée, M. **2005**. Thermodynamic characterization of metal dissolution and inhibitor adsorption processes in mild steel/ 2,5-bis(n-thienyl)-1,3,4-thiadiazoles/hydrochloric acid system. *Corrosion Science*, 47(12), pp: 2915–2931.

7. Khalil, N. **2003**. Quantum chemical approach of corrosion inhibition. *Electrochim. Acta*., 48(20), pp: 2635–2640.

8. Choa, P., Liang, Q. and Li, Y. **2005**. Electrochemical, SEM/EDS and quantum chemical study of phthalocyanines as corrosion inhibitors for mild steel in 1mol/l HCl. *Appl. Surf. Sci*., 252, pp: 1596-1607.

9. Xiao-Ci, Y., Hong, Z., Ming-Dao, L., Hong-Xuang, R. and Lu-An, Y. **2000**. Quantum chemical study of the inhibition properties of pyridine and its derivatives at an aluminum surface. *Corrosion Science*, 42, pp: 645-653.

10. Fontana, M.G. and Staehle, K.W. **1970**. *Advances in Corrosion Science and Technology*, Volume 1. Plenum, New York.

11. Udhayakala, P., Jayanthi, A. and Rajendiran, T.V. **2011**. Adsorption and quantum chemical studies on the inhibition potentials of some formazan derivatives. *Der Pharma Chemica*, 3(6), pp:528-539.

12. Ghailane, T., Balkhmima, R.A., Ghailane, R., Souizi, A., Touir, R., Ebn Touhami, M. and Marakchi, K.N. **2013**. Experimental and theoretical studies for mild steel corrosion inhibition in 1 M HCl by two new benzothiazine derivatives. *Corrosion Science*, 76, pp: 317–324.

13. Kandemirli, F. and Sagdinc, S. **2007**. Theoretical study of corrosion inhibition of amides and thiosemicarbazones. *Corrosion Science*, 49, pp:2118–2130.

14. Mert, B.D., Mert, M.E., Kardas, G. and Yazıcı, B. **2011**. Experimental and theoretical investigation of 3-amino-1,2,4-triazole-5-thiol as a corrosion inhibitor for carbon steel in HCl medium. *Corrosion Science*, 53, pp:4265–4272.

15. Issa, R. M., Awad, M.K. and Atlam, F.M. **2008**. Quantum chemical studies on the inhibition of corrosion of copper surface by substituted uracils. *Appl. Surf. Sci.*, 255(5), pp: 2433–2441.

16. Parr, R.G. and Yang, W. **1989**. *Density Functional Theory of Atoms and Molecules.* First Edition. Oxford University Press: New York.

17. Gece, G. **2008**. The use of quantum chemical methods in corrosion inhibitor studies. *Corrosion Science*,50, pp:2981–2992.

18. Ahamad, I., Prasad, R. and Quraishi, M.A. **2010**. Thermodynamic electrochemical and quantum chemical investigation of some schiff bases as corrosion inhibitors for mild steel in hydrochloric acid solutions. *Corrosion Science*, 52, pp: 933–942.

19. Kubba, R.M. and Abood, F.K. **2015.** DFT, PM3, AM1, and MINDO/3 quantum mechanical calculations for some INHC Cs symmetry Schiff bases as corrosion inhibitors for mild steel. *Iraqi Journal of Science*, 56(1C), pp: 602-621.

20. Ahmed, H.J. **2015**. Synthesis, characterization and study of antimicrobial activity of some new Schiff base derivatives containing 5-bromo isatin moiety. M.Sc. Thesis. Department of Chemistry, College of Science, University of Baghdad. Baghdad, Iraq.

21. Frisch, M.J. Trucks, G.W. Schlegel, H.B. Scuseria, G.E. Robb,M.A. Cheeseman, J.R. Montgomery, J.A. Jr., Vreven, T. Kudin, K.N. Burant, J.C. Millam, J.M. Iyengar, S.S. Tomasi, J. Barone, V. Mennucci, B. Cossi, M. Scalmani, G. Rega, N. Petersson, G.A. Nakatsuji, H. Hada, M. Ehara, M. Toyota, K. Fukuda, R. Hasegawa, J. Ishida, M. Nakajima, T. Honda, Y. Kitao, O. Nakai, H. Klene, M. Li, X. Knox, J.E. Hratchian, H.P. Cross, J.B. Bakken, V. Adamo, C. Jaramillo,J. Gomperts, R. Stratmann,R. E. Yazyev, O.Austin, A.J. Cammi,R. Pomelli,C Ochterski, J.W. Ayala, P.Y. Morokuma, K. Voth, G.A. Salvador, P. Dannenberg, J.J. Zakrzewski, V.G. Dapprich, S. Daniels, A.D. Strain, M.C. Farkas, O. Malick, D.K. Rabuck, A. D. Raghavachari, K Foresman, J.

B. Ortiz,J. V Cui, Q. Baboul, A. G. Clifford, S. Cioslowski, J. Stefanov, B.B. Liu, G. Liashenko, A. Piskorz, P. Komaromi, I. Martin, R.L. Fox, D.J. Keith, T. Al-Laham, M.A. Peng, C.Y. Nanayakkara, A. Challacombe, M. Gill, P.M. W. Johnson B. Chen, W. Wong, M.W. Gonzalez, C.and Pople, J.A. **2003.** *Gaussian 03*, Gaussian. Inc. Pittsburgh PA.

22. Becke, A.D. **1993**. Density-functional thermochemistry. III. The role of exact exchange. *J. Chem. Phys.*, 98, pp: 5648-5652.

23. Ee, C., Yang, W. and Parr, R.G. **1988**. Development of the Colle-Salvetti correlation-energy formula into a functional of the electron density. *Phys. Rev*., B 41, pp: 785-789.

24. a-Fang, J. and Li, J. **2002.** Quantum chemistry study on the relationship between molecular structure and corrosion inhibition efficiency of amides. *J. Mol. Struct*.: *THEOCHEM*, 593, pp: 179-185. b- Fleming, I. **1976.** *Frontier Orbitals and Organic Chemical Reactions*. John Wiley and Sons, NewYork.

25. Zhang, J., Liu, J., Yu, W., Yan, Y., You, L. and Liu, L. **2010**. Molecular modeling of the inhibition mechanism of 1-(2-aminoethyl)-2-alkyl-imidazoline. *Corrosion Science*, 52, pp: 2059-2065.

26. Koopmans, T. **1933**. Über die zuordnung von wellenfunktionen und eigenwerten zu den einzelnen elektronen eines toms. *Physica*., 1, pp: 104-113.

27. Rauk, A. **2001**. *Orbital Interaction Theory of Organic Chemistry*. Second Edition. John Wiley & Sons: NewYork.

28. Pearson, R.G. **1988**. Absolute electronegativity and hardness application to inorganic chemistry. *Inorganic Chemistry*, 27(4), pp: 734-740.

29. Parr, R.G. and Pearson, R.G. **1983**. Absolute hardness: companion parameter to absolute electronegativity. *J. Am. Chem. Soc.*, 105, pp: 7512-7516.

30. Parr, R.G., Donnelly, R.A., Levy, M. and Palke, W.E. **1978**. Empirical evaluation of chemical hardness. *J. Chem. Phys.*, 68, pp: 3801-3807.

31. Chermette, H. **1999**. Chemical reactivity indexes in density functional theory. *J. Comput. Chem.*, 20, pp: 129-154

32. Lukovits, I., Kálmán, E. and Zucchi, F. **2001.** Corrosion inhibitors—correlation between electronic structure and efficiency. *Corrosion*, 57, pp:3-9.

33. Wang, H., Wang, X., Wang, H., Wang, L. and Liu, A. **2007**. DFT study of new bipyrazole derivatives and their potential activity as corrosion inhibitors. *Journal of Molecular Modeling*,13(1), pp: 147-153.

34. Zhao, P., Liang, Q. and Li, Y. **2005**. Electrochemical, SEM/ EDS and quantum chemical study of phthalocyanines as corrosion inhibitors for mild steel in 1 mol/l HCl. *Applied Surface Science*, 252(5), pp: 1596-1607.

35. Popova, A., Christov, M. and Deligeorigiev, T. **2003**. Influence of the molecular structure on the inhibitor properties of benzimidazole derivatives on mild steel corrosion in 1 M hydrochloric acid. *Corrosion*, 59, pp:756–764.

36. Kubba, R.M. and Abood, F.K. **2015**. Quantum chemical investigation of some schiff bases as corrosion inhibitors for mild steel in hydrochloric acid solutions. *Iraqi Journal of Science*,56(2B), pp: 1241-1257.

37. Al-jeilawi, O.H. **2013**. Synthesis of some organic compounds as corrosion inhibitors in petroleum industry. Ph.D. Thesis. Department of Chemistry, College of Science, University of Baghdad. Baghdad, Iraq.

38. Stoyanova, A., Petkova, G. and Peyerimhoff, S.D. **2002**. Correlation between the molecular structure and the corrosion inhibiting effect of some pyrophthalone compounds. *Chem. Phys*., 279, pp: 1-6.

39. Rodriguez-Valdez, L., Martinez-Villafane, A. and Glossman-Mitnik, D. **2005**. CHIH-DFT theoretical study of isomeric thiatriazoles and their potential activity as corrosion inhibitors. *J. Mol. Struct.: THEOCHEM,*716, pp: 61-65.

40. Li, X., Deng, S., Fu, H. and Li, T. **2009**. Adsorption and inhibition effect of 6-benzylaminopurine on cold rolled steel in 1.0 M HCl. *Electrochimica Acta*., 54(16), pp: 4089-4098.

41. Obi-Egbedi, N.O., Obot, I.B., El-Khaiary, M.I., Umoren, S.A. and Ebenso, E.E. **2011**. Computational simulation and statistical analysis on the relationship between corrosion inhibition efficiency and molecular structure of some phenanthroline derivatives on mild steel surface. *Int. J. Electro Chem., Sci.*, 6(11), pp: 5649-5675.